New Journal of Physics
The open-access journal for physics

Towards sympathetic cooling of large molecules: cold collisions between benzene and rare gas atoms

P Barletta[1], **J Tennyson and P F Barker**
Department of Physics and Astronomy, University College London, Gower Street, London WC1E 6BT, UK
E-mail: p.barletta@ucl.ac.uk

New Journal of Physics **11** (2009) 055029 (12pp)
Received 15 December 2008
Published 14 May 2009
Online at http://www.njp.org/
doi:10.1088/1367-2630/11/5/055029

Abstract. This paper reports on calculations of collisional cross sections for the complexes X–C_6H_6 ($X = {}^3$He, ^{4}He, Ne) at temperatures in the range 1 μK–10 K and shows that relatively large cross sections in the 10^3–10^5 Å^2 range are available for collisional cooling. Both elastic and inelastic processes are considered in this temperature range. The calculations suggest that sympathetically cooling benzene to microkelvin temperatures is feasible using these co-trapped rare gas atoms in an optical trap.

Contents

1. Introduction

The creation of ultra-cold and chemically stable molecular gases below millikelvin temperatures is currently an important goal in cold molecular physics. In this largely unexplored temperature regime for molecules, chemical reactions are dominated by tunneling and resonance phenomena which can lead, for example, to an increase in reaction rates as the temperature is decreased [1]. Furthermore, when the kinetic energy of dipolar molecules becomes comparable with their

[1] Author to whom any correspondence should be addressed.

interaction energy, their long-range and anisotropic interactions are predicted to lead to a variety of novel quantum phases [2]. The ability to trap ultra-cold molecules for long periods offers a unique environment for high-resolution spectroscopy. This capability allows the testing of time variation in fundamental constants [3], precision tests of physics beyond the standard model [4] and parity violation at the molecular level [5].

Ultra-cold heteronuclear and homonuclear diatomic molecules can be created from laser cooled alkali metal atoms using photo association and by association on Feshbach resonances. In these schemes, both cold polar and non-polar species have been produced in excited vibrational states. Recent work has shown that these highly excited species can be promoted to their absolute ground state with high efficiency [6]. The range of ultra-cold molecular species created in this way is however limited to the relatively few species that can be laser cooled and trapped; therefore, other methods have been developed to produce more complex diatomic and polyatomic species which are chemically stable. Typical techniques are Stark [7] and Zeeman [8] deceleration which produce stationary molecular ensembles in a single quantum state within the ground vibrational state. Another method, called the buffer gas cooling, uses thermalizing collisions between paramagnetic molecules and cold atoms to produce cold, magnetically trapped molecules at temperatures greater than 100 mK [9]. These methods, while relatively general, are limited to the creation of gases at temperatures in excess of 10 mK and thus further cooling is required to reach the microkelvin (μK) temperature range.

A promising route for cooling to microkelvin temperatures is to extend the buffer gas cooling technique by using colder, laser-cooled atomic species which can be created in the (μK) range. This technique requires thermalizing elastic collisions between the atom and a cold molecular species that is for example created by Stark deceleration. This method is used to sympathetically cool a number of atomic species which cannot be laser cooled to low temperatures [10]. The possibility of sympathetic cooling molecules via this route has been explored theoretically by considering ultra-cold and cold collisions between molecules that can be electrostatically Stark decelerated and laser-cooled alkali metal atomic species. These studies have considered co-trapping in magnetic [11] and electric [12] traps; they indicate that at some temperatures over the cooling range required, inelastic processes dominate over elastic collisions. These inelastic processes lead to trap loss as molecules are promoted to untrappable states preventing further cooling. Additionally, reactions between collision partners can occur which reduce the number of molecular species available for sympathetic cooling [13].

To explore the sympathetic cooling of optical Stark decelerated non-polar species [14, 15] within an optical trap we have recently studied cold and ultra-cold collisions between molecular hydrogen and ultra-cold laser-cooled rare gas atoms [16, 17]. Our results have established that sympathetic cooling of a simple diatomic species, such as molecular hydrogen, is feasible a with range of the rare gas atoms, and that based on the calculated elastic cross sections, cooling times of less than a second would be required to reach microkelvin temperatures. Co-trapping both species within an optical trap is important for sympathetic cooling because in principle all species and all ground state ro-vibrational states can be trapped, thus preventing trap losses even if state changing inelastic collisions occur. In addition, the use of rare gas atoms as the collision partners minimizes the likelihood of reaction between the molecular species and atomic species.

In the present paper, we consider low-temperature collisions between cold and ultra-cold rare gas atoms and benzene molecules to evaluate the sympathetic cooling of benzene molecules. We assume that the rare gas atoms are produced following laser cooling in their metastable state and quenched to their absolute ground state. Benzene is a prototypical example

of a more complex molecular species that can, in principle, be loaded into an optical trap using optical Stark deceleration. Importantly, it has been optically Stark decelerated [14, 18] and because it has a significantly larger polarizability, it is more efficiently trapped than molecular hydrogen. It is also interesting when compared to molecular hydrogen, because the collisional interactions are more anisotropic and inelastic channels might become important at the upper range of the temperatures we consider for sympathetic cooling.

The benzene–rare gas complexes have drawn significant attention, both experimentally and theoretically, as prototype systems for the study of intermolecular forces between aromatic molecules and non-polar species [19]. In particular, the scientific interest resides in modeling the interaction of aromatic π-systems, which controls several biological phenomena, such as the tertiary structure of proteins or the vertical base–base interaction in DNA. Most works, both theoretical and experimental, have concentrated on the benzene–argon complex. Brocks *et al* [20] provided a general strategy for solving the quantum dynamical problem of two semi-rigid interacting polyatomic fragments. Subsequently, Brocks and Huygen [21] implemented this method to study bound states of benzene–argon. Related work on this system has been performed by van der Avoird and co-workers [22]–[24]. Highly accurate *ab initio* studies of the van der Waals interaction for benzene–argon were carried out by Koch *et al* [25, 26], and by Klopper and *et al* [27]. Benzene–helium was investigated by Koch and co-workers [28]. Recently, Pirani *et al* [29]–[31] produced potential energy surfaces (PESs) for all five benzene–rare gas complexes which combine previous spectroscopic measurements with the analysis of collisions in supersonic expansions.

The paper is organized as follows. Section 2 presents the computational methods used in this study, section 3 describes the main results and the last section is devoted to the conclusions.

2. Numerical procedure

Following Brocks and Huygen [21], we use body-fixed coordinates to describe the benzene–rare gas dimer. The system Hamiltonian H can be split into two terms

$$H = H_{C_6H_6} + H_{\text{int}}, \tag{1}$$

where $H_{C_6H_6}$ is the isolated benzene Hamiltonian, and H_{int} reads [20]

$$H_{\text{int}} = \frac{1}{2\mu R^2}(J^2 + j^2 - 2\mathbf{j}\cdot\mathbf{J}) - \frac{1}{2\mu R}\frac{d^2}{dR^2}R + V_{\text{int}}, \tag{2}$$

where R is the distance between the benzene center-of-mass and the rare gas atom, μ is the benzene–atom reduced mass, J is the total angular momentum of the complex and j the angular momentum of the benzene molecule. V_{int} is the benzene–atom interaction potential, which we discuss below. Five angles are necessary in order to define a coordinate system embedded on the benzene. We therefore define an angular basis element as

$$|k, \Omega, M, j, J\rangle = D^j_{k,\Omega}(\phi, \theta, \gamma) D^J_{\Omega,M}(0, \beta, \alpha), \tag{3}$$

where D is a Wigner rotation function, M is the projection of J on the space fixed z-axis, Ω is the projection of both J and j on the body fixed z-axis and k is the projection of j on the benzene fixed z-axis. Brocks and Huygen [21] also detail how to construct a basis invariant under particle permutation. In this work, we restrict our analysis to the case $J = 0$, which implies $M = \Omega = 0$. We also employ a rigid rotor approximation for the benzene molecule. With this assumption the

Table 1. Irreducible representations of the angular basis of equation (5). The first column reports the irrep $\Gamma(\mathrm{D}_{6h})$ of the angular basis element in column 2. The energies and quantum numbers jk ($k > 0$) of the two lowest benzene states associated with each basis subset are reported in the last four columns. Energies are in cm^{-1}. Columns 1–5 are taken from Brocks and Huygen [21]. Note that the states defined in column 2 are not normalized.

Rot. Symm.	Basis	j	k	$\Gamma(C_{6v})$	Spin. Symm.	Spin	Parity	E_0	(jk)	E_1	(jk)
A_{1g}	$\|j,k\rangle + \|j,-k\rangle$	Even	0, 6, 12, ...	A_1	B_1	0,2	+	0.000	(00)	1.138	(20)
A_{2g}	$\|j,k\rangle - \|j,-k\rangle$	Even	6, 12, ...	A_2	B_2	1	+	4.554	(66)	0.247	(86)
B_{1g}	$\|j,k\rangle + \|j,-k\rangle$	Odd	3, 9, 15, ...	B_2	A_2	0	+	1.423	(33)	4.839	(53)
B_{2g}	$\|j,k\rangle - \|j,-k\rangle$	Odd	3, 9, 15, ...	B_1	A_1	1,3	+	1.423	(33)	4.839	(53)
E_{1g}	$\|j,k\rangle, \|j,-k\rangle$	Odd	1, 5, 7, 11, ...	E_1	E_2	1,2	+	0.285	(11)	2.182	(31)
E_{2g}	$\|j,k\rangle, \|j,-k\rangle$	Even	2, 4, 8, 10, ...	E_2	E_1	0,1,2	+	0.759	(22)	4.914	(42)
A_{1u}	$\|j,k\rangle - \|j,-k\rangle$	Odd	0, 6, 12, ...	A_2	B_2	1	−	0.380	(10)	2.277	(30)
A_{2u}	$\|j,k\rangle + \|j,-k\rangle$	Odd	6, 12, ...	A_1	B_1	0,2	−	7.211	(76)	13.662	(96)
B_{1u}	$\|j,k\rangle - \|j,-k\rangle$	Even	3, 9, 15, ...	B_2	A_2	0	−	2.941	(43)	7.116	(63)
B_{2u}	$\|j,k\rangle + \|j,-k\rangle$	Even	3, 9, 15, ...	B_1	A_1	1,3	−	2.941	(43)	7.116	(63)
E_{1u}	$\|j,k\rangle, \|j,-k\rangle$	Even	1, 5, 7, 11, ...	E_1	E_2	1,2	−	1.044	(21)	3.700	(41)
E_{2u}	$\|j,k\rangle, \|j,-k\rangle$	Odd	2, 4, 8, 10, ...	E_2	E_1	0,1,2	−	1.898	(32)	5.313	(52)

basis elements (3) are also eigenstates of the benzene Hamiltonian $H_{\mathrm{C_6H_6}}$ with energies

$$E_{jk} = Bj(j+1) + (C-B)k^2, \tag{4}$$

where we use the lamina rule to set $C \approx B/2$, with $B = 0.189\,75\ \mathrm{cm}^{-1}$ for the vibrational ground state. For $J = 0$, it is only necessary to consider the internal degrees of freedom of the complex which can be represented using three coordinates, the benzene–atom distance R and the benzene orientation angles θ, ϕ, representing, respectively, the latitude and longitude.

Table 1 illustrates the different irreducible representations (irreps) in which the angular basis can be divided starting from the basis elements of equation (3). For simplicity, the shorthand notation

$$|j,k\rangle = D^j_{k,0}(\phi,\theta,0) \tag{5}$$

has been introduced. The good quantum numbers for the benzene–atom dimer are thus the benzene nuclear spin S, its irrep Γ_S (note that the same S appears in different Γ_S, and that each Γ_S can contain more than one S), and the parity (which is also given by $(-1)^{j+k}$). $\mathrm{D_{6h}}$ group labels, given in the first column of table 1, will be used for simplicity. Note that states corresponding to the same irrep, but with different spins, are completely degenerate since we neglect any term depending on nuclear spin in both the benzene internal potential and the benzene–atom potential. The nuclear spin degrees of freedom of benzene are not consider explicitly in the dynamics but only for determining the irrep of the different benzene rotational levels and their multiplicity.

The benzene rotational–vibrational ground state has A_{1g} symmetry. Table 1 also reports the two lowest energy levels of benzene associated with each irrep. The threshold energy at which the lowest inelastic channel opens thus depends on the particular irrep considered. In particular,

the irrep A_{1g} has the lowest threshold. Note that these energies correspond to the center-of-mass frame. When the scattering energy is defined in the laboratory frame a scaling factor needs to be introduced, which reduces the energy available in the collision in the center-of-mass frame. Our calculations will consider benzene in its ground state and will be thus restricted to the first irrep of table 1.

The normalized angular basis for the irrep A_{1g} can be written as

$$|j, k, A_{1g}\rangle = \frac{1}{\sqrt{2(1+\delta_{k0})}} \left(|j, k\rangle + |j, -k\rangle\right), \tag{6}$$

where the angular element is assumed to be normalized

$$\langle j', k'|j, k\rangle = \delta_{j,j'}\delta_{k,k'}. \tag{7}$$

The system wavefunction is then expanded on the basis of equation (6)

$$\Psi = \sum_{jk} f_{jk}(R)/R|k, j, A_{1g}\rangle, \tag{8}$$

where the set of functions $\{f_{jk}\}$ are the unknown of the problem. They can be determined by solving an infinite system of coupled equations which will be discussed in the next section. In order to calculate the coupling terms, let us first expand the benzene–atom potential on the following basis:

$$V(R, \theta, \phi) = \sum_{lm} v_{lm}(R) \sqrt{\frac{(2l+1)}{4\pi}} \sqrt{\frac{(l-m)!}{(l+m)!}} P_l^m(\cos\theta) \cos(m\phi), \tag{9}$$

where P_l^m is an associated Legendre function. As a consequence of the structure of benzene, the benzene–atom potential $V(R, \theta, \phi)$ is symmetric under reflection in the $\theta = \pi/2$ plane, and under rotations of multiples of $\pi/3$ around the $\theta = 0$ axis. Consequently, only terms with l even and $m = 6n$ ($n = 0, 1, 2, \ldots$) are nonzero in the expansion of equation (9). The potential energy matrix element between two angular basis vectors is readily evaluated

$$V_{jk,j'k'} = \langle j, k, A_{1g}|V|j', k', A_{1g}\rangle = \sum_{lm} c_{lm}^{jkj'k'} v_{lm}(R), \tag{10}$$

where the coupling coefficients c_{lm} are

$$c_{lm}^{jkj'k'} = \sqrt{\frac{(2j+1)(2j'+1)(2l+1)}{4\pi}} \begin{pmatrix} j & l & j' \\ 0 & 0 & 0 \end{pmatrix} \left[\begin{pmatrix} j & l & j' \\ -k & -m & -k' \end{pmatrix} + \begin{pmatrix} j & l & j' \\ -k & -m & k' \end{pmatrix} + \begin{pmatrix} j & l & j' \\ -k & m & -k' \end{pmatrix} + \begin{pmatrix} j & l & j' \\ -k & m & k' \end{pmatrix} \right]. \tag{11}$$

In the sum of equation (10) the indices j, j', l must obey standard triangular limits, whereas, as it can be seen from equation (11), only four values of m are allowed for each pair k, k', such as $m = -k - k', k - k', k' - k, k + k'$. Following Brocks *et al* [20], the matrix elements of the kinetic energy operator of equation (2) can also be readily evaluated yielding the following system of coupled one-dimensional differential equations:

$$\left[-\frac{1}{2\mu}\frac{d^2}{dR^2} + E_{jk} - E\right] f_{jk} + \sum_{j'k'} V_{jk,j'k'} f_{j'k'} = 0, \tag{12}$$

where the number of coupled equations is equal to the number of terms in the expansion of equation (8). The possible values for $\{j', k'\}$ depend on the number of terms used in the expansion of the potential in equation (10). As we will consider benzene in its ground state, only terms with $k' \leqslant m_{\max}$ will enter in equation (12), where $m_{\max}$ is the maximum value of m used in expanding the potential.

3. Results

The PESs used in this work are those by Pirani *et al* [31]. They represent the benzene–rare gas interactions using a simple analytical form written as a sum of atom–bond interaction contributions, and whose parameters were fitted from experimental and *ab initio* data. Those surfaces are also freely available from the web [32]. The PESs were then expanded into the basis of equation (9) using a Gauss–Legendre formula with 1000 points in θ and a seven-point Lagrange formula with 1000 points uniformly distributed in ϕ. The functions $v_{lm}(R)$ were thus calculated on a uniform grid in the range 0.01–200 Å, with a step of 0.01 Å. The expansion was restricted to $m_{\max} = 0$. Consequently, the expansion for the wavefunction in equation (8) contains the channels $\{0, 0\}$, $\{2, 0\}$, $\{4, 0\}$, ... A cut of $10^8\,\mathrm{cm}^{-1}$ was imposed to the benzene–atom potential in order to avoid numerical problems.

The system of coupled equations (12) has been solved using a log-derivative propagator scheme [33, 34]. The large number of vibrational states present in these van der Waals dimers makes the use of a polynomial expansion for the $\{f_{jk}\}$ functions computationally difficult therefore we used a numerical procedure. The R coordinate has been parametrized using a uniformly distributed grid from 0.01 to 300 Å, with a step of 0.01 Å. The numerical stability of the results has been checked in the range 200–300 Å, and by changing the grid step in the range 0.1–0.001 Å. The stability of the results against the choice of the initial point R_0 where to start the propagation was also checked and a value of $R_0 = 1.5$ Å was selected. Finally, the convergence with the number of closed channels has been checked at four different scattering energies, $E = 10^{-6}$, 10^{-4}, 10^{-2} and $1\,\mathrm{cm}^{-1}$. The correctness of the procedure employed was further checked repeating the same calculations using the MOLSCAT package [35], showing substantial agreement. The scattering observables, such as the K matrix, are extracted by the long-range part of the set of functions $\{f_{jk}(R)\}$ following the Johnson's recipe [33]. Table 2 reports the convergence in terms of the closed channels for the K matrix for the benzene–neon complexes. The dimension of the matrix is equal to the number of open channels. Therefore, at energies below the first threshold the K matrix reduces simply to a scalar. Above the threshold it becomes a true 2×2 matrix. The S matrix is then obtained as

$$S = (I - \mathrm{i}K)^{-1}(I + \mathrm{i}K), \tag{13}$$

where I is the identity matrix.

The experimental conditions we are interested in reproducing assume that the rare gas atom is at rest in the laboratory frame, and therefore essentially all the scattering energy is the kinetic energy of the impinging benzene molecule. With this assumption, and due to the heavy mass of benzene, it is easy to show that only a small portion of the original scattering energy can be used inelastically in the center-of-mass frame. In fact, the energy available in the center-of-mass frame is connected to the laboratory energy by the factor χ

$$\chi = \frac{m_X}{m_X + m_{\mathrm{C_6H_6}}}, \tag{14}$$

Table 2. Convergence for the K_{11} matrix element at four different scattering energies in the center-of-mass frame, for the benzene–Ne complex. N is the number of closed channels considered. The highest benzene state considered in this expansion is {20, 0} which has an energy of 281 cm^{-1}.

					1.145 (cm^{-1})	
N	10^{-6} (cm^{-1})	10^{-4} (cm^{-1})	10^{-2} (cm^{-1})	10^{0} (cm^{-1})	K_{11}	K_{12}
4	0.012 086 99	0.122 563 33	4.870 043 21	−0.884 131 15	1.440 372 41	0.237 464 36
6	0.012 673 41	0.128 451 27	6.068 451 97	1.306 775 65	2.687 592 29	0.444 136 56
8	0.005 413 39	0.056 406 58	1.532 677 31	0.058 626 60	0.324 452 72	−0.187 559 72
10	−0.021 394 82	−0.195 305 84	0.361 095 78	0.361 753 11	1.793 642 04	0.421 743 66
12	−0.107 812 67	−0.878 780 59	0.063 092 19	5.253 779 98	1.446 449 97	0.474 103 91
14	−0.147 815 91	−1.142 412 65	0.032 114 95	3.739 022 23	1.359 878 72	0.491 966 36
16	−0.151 314 94	−1.164 155 66	0.030 109 13	3.664 395 90	1.352 108 42	0.493 522 71
18	−0.151 497 43	−1.165 284 19	0.030 006 69	3.660 873 28	1.351 651 19	0.493 607 41
20	−0.151 505 70	−1.165 335 38	0.030 002 04	3.660 724 49	1.351 628 73	0.493 611 39

Table 3. X–C_6H_6 scattering parameters. The second column reports the percentage of laboratory energy available in the center-of-mass frame, assuming that the rare gas atom is at rest in the laboratory frame. The third column reports the first threshold energy in the laboratory frame. Scattering length (a_S) and effective range (r_{eff}), in Å, are given in the fourth and fifth columns, respectively.

X	χ	ΔE (K)	a_s (Å)	$\lvert r_{eff}\rvert$ (Å)
^{3}He	3.72	45.75	−15.21	9.28
^{4}He	4.87	34.95	−4.60	44.6
Ne	20.53	8.29	155.80	40.9

where m_X and $m_{C_6H_6}$ are the masses of the atom and benzene, respectively. Table 3 reports the values of χ for the different complexes. The threshold ΔE for the first inelastic channel is then recalculated in terms of the laboratory scattering energy. As expected from equation (14) the effect is the more pronounced for atoms of smaller mass. In particular, for ^{3}He, for inelastic collisions to occur the scattering energy in the laboratory frame about 50 times bigger than the energy gap in benzene is required. This effect is reduced for heavier atoms but it still introduces a significant factor, the lowest being 1.6 for benzene–xenon. The last two columns of table 3 report the scattering length a_S and the effective range r_{eff} extracted from the phase shifts. As these quantities were not directly calculated, their associated uncertainty is significant, particularly to the effective range where it is estimated to be about 5%.

Table 4 reports the contributions of the s- and p-waves to the total cross section, for two incident energies in the center-of-mass frame. The results of this table were obtained using the MOLSCAT package [35]. Whereas the contribution of the p-wave for the higher energy is rather large, for the lower energy the cross section is dominated by the s-wave. As for Ne–benzene the lower incident energy of 0.01 cm^{-1} happen to be near a minimum of the cross section, for this system we have calculated the p-wave contribution to the cross section at a third lower energy. The table also reports the value of the classical turning point r_J defined as $r_J = r_{cl}\sqrt{J(J+1)}$, and $r_{cl} = \sqrt{\hbar^2/2\mu E}$.

Table 4. Contribution of the s- and p-waves to the total cross sections at selected incident energies in the center-of-mass frame. The last row reports the classical turning point for the channel $J = 1$.

	^{3}He		^{4}He		Ne		
E (cm^{-1})	0.01	1	0.01	1	0.0001	0.01	1
$\sigma(s)$ (Å^2)	2500	41	330	40	76000	1	13
$\sigma(p)$ (Å^2)	150	51	1	70	3	900	21
r_{cl} (Å)	24.1	2.41	21.0	2.10	103	10.3	1.03
r_1 (Å)	34.1	3.41	29.8	2.98	145	14.5	1.45

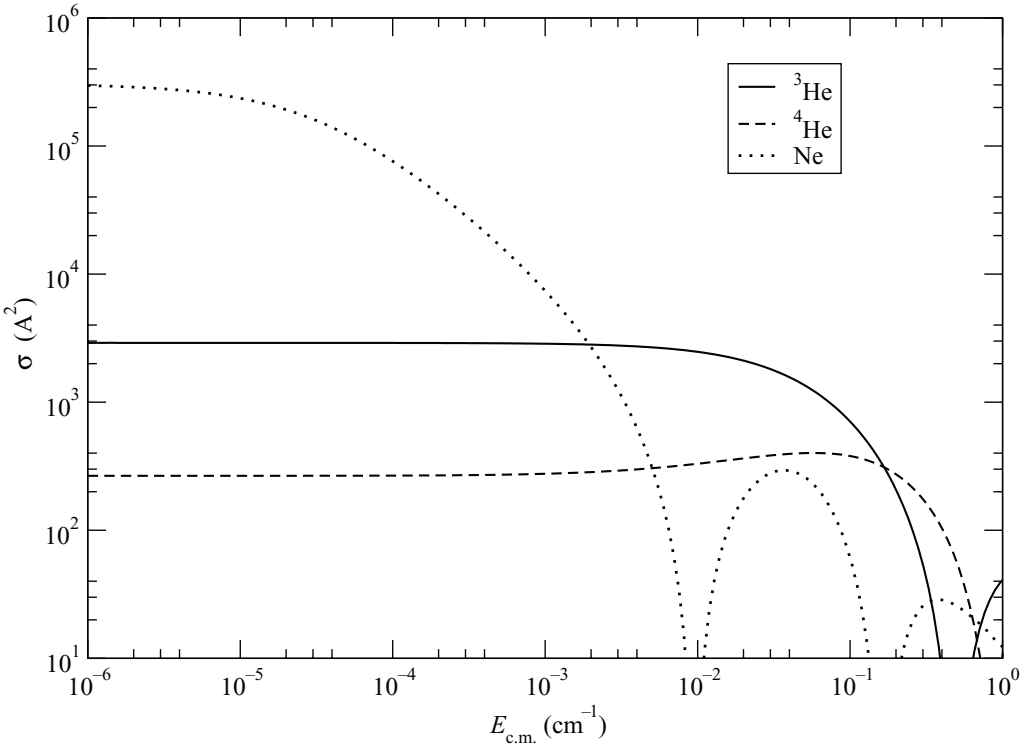

Figure 1. Collisional cross sections for benzene–rare gas atom complexes over the energy range from 1 μ cm^{-1} to 1 cm^{-1}, in the center-of-mass frame.

Figure 1 shows the elastic cross section for the three complexes ^{3}He–C_6H_6, ^{4}He–C_6H_6 and Ne–C_6H_6, as a function of the center-of-mass energy, in the range of 10^{-6}–1 cm^{-1}. The cross sections are constant over a considerable range of scattering energies, up to 20 mK, and their magnitude is comparable to those used in sympathetic cooling of experiments between alkalis [10]. The elastic cross sections for ^{3}He and ^{4}He differ at low energies by an order of magnitude, as a consequence of the substantially different mass of the two isotopes. In similar works, on other molecules [17, 36, 37], a qualitatively similar behavior was also reported.

Figure 2 shows two elements of the S matrix for the Ne–C_6H_6 complex. The diagonal $|S_{11}|^2$ and off-diagonal $|S_{12}|^2$ elements are plotted as a function of the scattering energy (in kelvin) in the laboratory frame, where the state labelled 1 refers to the rotational ground

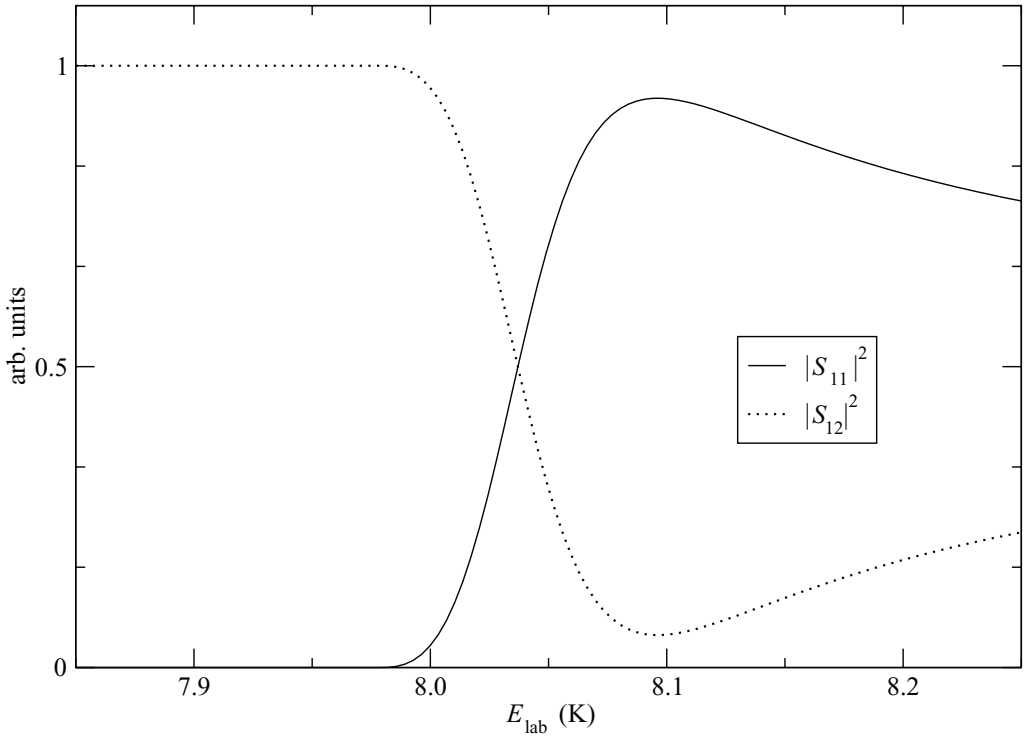

Figure 2. Diagonal and off-diagonal elements for the S matrix just above the first threshold, for Ne–C_6H_6. The matrix elements are plotted as functions of the scattering energy, in K, in the laboratory frame, differently from the other figure and tables, where the scattering energy was given in cm^{-1} and in the center-of-mass frame.

state of benzene (0, 0), and the state 2 to the first excited state in the A_{1g} irrep (2, 0). Below 6 K $|S_{12}|^2$ is zero as there is insufficient energy to excite benzene to the higher rotational level. In practice, the excitation probability remains very low up to 8 K. A higher threshold should be assumed for benzene–helium due to the lower χ factor for those complexes. In fact, the rapid rise in the inelastic cross section near threshold displayed in figure 2 is probably associated with a resonance; this will be investigated fully in future work.

4. Discussion and conclusions

The present paper presents calculations of benzene–rare gas atom cross sections which are of importance for sympathetic cooling of benzene in an optical trap. The analysis of this work has been restricted to the A_{1g} symmetry block. As the experimental set up will possibly produce benzene not just in the absolute ground state, but also in other nuclear spin states and hence symmetries, our analysis of the cross section should consequently also be extended to consider them. However, we note that the lowest spin allowed excitation is actually for the A_{1g} symmetry considered in this work. We therefore anticipate even fewer problems with losses due to inelastic collisions for these other nuclear spin isotopomers, collisions for which will be considered in future work.

A number of approximations have been introduced in order to reduce the numerical difficulty of the problem. In particular, the expansion basis for the benzene has been restricted to the lowest vibrational band, the benzene–atom potential expansion has been limited to the term $m = 0$ (the next nonzero term is $m = 6$), and, finally, the calculation of the scattering observables has been limited to the $J = 0$ contribution. The first approximation is sound since from table 2 it can be seen that the highest states considered have a lower energy than the first excited benzene vibrational band, which is at more than 400 cm^{-1} above the ground state. The other two approximations can be easily relaxed, and a more systematic investigation where more expansion functions in the potential are included, as well as the contribution from $J > 0$, will also be carried out shortly. This work represents a first step towards a systematic analysis of benzene–rare gas atom collisions at ultra-cold temperature. The extension of this work to include the heavier rare gas atoms (Ar, Kr and Xe) is under way.

In a previous paper [17], we have considered the complexes X–H_2, and the different cross section were analyzed in terms of the bound states of each complex. A similar analysis for benzene is not as straightforward because of the large number of vibrational states possible in benzene–rare gas atom dimers. However, the scattering lengths for those systems are large below a temperature of 20 mK, indicating that sympathetic cooling is feasible for benzene molecules that have been optically Stark decelerated into an optical trap. In addition, inelastic processes do not appear to be important for collision energies corresponding to temperatures of less than 8 K, which is well above temperatures (< 150 mK) at which sympathetic cooling would begin in an optical trap.

Finally, we note that a problem normally associated with ultra-cold scattering calculations is their strong dependence on the PES employed [17]. It will be interesting to repeat the analysis of rare gas–benzene collisions considering different PESs available in the literature. In addition, it is anticipated that PES will be modified by a small amount within an optical trap and this effect has not been included in this work. However, our computed elastic cross sections are large and even a significant reduction, by up to an order of magnitude, would not preclude sympathetic cooling of benzene by means of laser-cooled and -trapped rare gas atoms.

References

[1] Balakrishnan N and Dalgarno A 2001 Chemistry at ultracold temperatures *Chem. Phys. Lett.* **341** 652
[2] Micheli A, Brennen G K and Zoller P 2006 A toolbox for lattice–spin models with polar molecules *Nat. Phys.* **2** 341
[3] Hudson E R, Lewandowski H J, Sawyer B C and Ye J 2006 Cold molecule spectroscopy for constraining the evolution of the fine structure constant *Phys. Rev. Lett.* **96** 143004
[4] Hudson J J, Sauer B E, Tarbutt M R and Hinds E A 2002 Measurement of the electron electric dipole moment using YbF molecules *Phys. Rev. Lett.* **89** 023003
[5] Bast R and Schwerdtfeger P 2003 Parity-violation effects in the c-f stretching mode of heavy-atom methyl fluorides *Phys. Rev. Lett.* **91** 023001
[6] Ni K K, Ospelkaus S, de Miranda M H G, Pe'er A, Neyenhuis B, Zirbel J J, Kotochigova S, Julienne P S, Jin D S and Ye J 2008 A high phase-space-density gas of polar molecules *Science* **322** 231
[7] Bethlem H L, van Roij A J A, Jongma R T and Meijer G 2002 Alternate gradient focusing and decelerating of a molecular beam *Phys. Rev. Lett.* **88** 133033
[8] Vanhaecke N, Meier U, Andrist M, Meier B H and Merkt F 2007 Multistage zeeman deceleration of hydrogen atoms *Phys. Rev.* A **75** 031402

[9] Weinstein J D, de Carvalho R, Guillet T, Friedrich B and Doyle J M 1998 Magnetic trapping of calcium monohydride molecules at millikelvin temperatures *Nature* **395** 148
[10] Mosk A, Kraft S, Mudrich M, Singer K, Wohlleben W, Grimm R and Weidemuller M 2001 Mixture of ultracold lithium and cesium atoms in an optical dipole trap *Appl. Phys.* B **73** 793
[11] Lara M, Bohn J L, Potter D E, Soldán P and Hutson J M 2006 Ultracold Rb–OH collisions and prospects for sympathetic cooling *Phys. Rev. Lett.* **97** 183201
[12] Zuchowski P S and Hutson J M 2008 Prospects for producing ultracold NH_3 molecules by sympathetic cooling: a survey of interaction potentials *Phys. Rev.* A **78** 022701
[13] Soldán P and Hutson J M 2004 Interaction of $NH(X^3\Sigma^-)$ molecules with rubidium atoms: implications for sympathetic cooling and the formation of extremely polar molecules *Phys. Rev. Lett.* **92** 163202
[14] Fulton R, Bishop A I and Barker P F 2004 Optical stark decelerator for molecules *Phys. Rev. Lett.* **93** 243004
[15] Fulton R, Bishop A I, Shneider M N and Barker P F 2006 Controlling the motion of cold molecules with deep periodic optical potentials *Nat. Phys.* **2** 465
[16] Barletta P, Tennyson J and Barker P F 2008 Creating ultracold molecules by collisions with ultracold rare gas atoms in an optical trap *Phys. Rev.* A **78** 052707
[17] Barletta P 2009 Comparative study of rare gas-H_2 triatomic complexes *Eur. Phys. J.* D accepted for publication
[18] Fulton R, Bishop A I, Shneider M N and Barker P F 2006 Optical stark deceleration of nitric oxide and benzene molecules using optical lattices *J. Phys. B: At. Mol. Opt. Phys.* **39** S1097–109
[19] Hobza P, Selzle H L and Schlag W 1994 Structure and properties of benzene-containing molecular clusters: nonempirical *ab initio* calculations and experiments *Chem. Rev.* **94** 1767–85
[20] Brocks G, van der Avoird A, Sutcliffe B T and Tennyson J 1983 Quantum dynamics of non-rigid systems comprising two polyatomic molecules *Mol. Phys.* **50** 1025–43
[21] Brocks G and Huygen T 1986 Van der Waals rovibrational states of atom–molecule complexes: Ar–benzene and Ar–tetrazine *J. Chem. Phys.* **85** 3411–24
[22] van der Avoird A 1993 Van der Waals rovibrational levels and the high resolution spectrum of the argon–benzene dimer *J. Chem. Phys.* **98** 5327–36
[23] Riedle E and van der Avoird A 1996 Unambigous assigment of the van der Waals modes of benzene–Ar by analysis of the rotationally resolved UV-spectra and comparison with multidimensional calculations *J. Chem. Phys.* **104** 882–98
[24] Neushaser R, Braun J, Neusser H J and van der Avoird A 1998 Vibrational overtones in the electronic ground state of the benzene–Ar complex: a combined experimental and theoretical analysis *J. Chem. Phys.* **108** 8408–17
[25] Koch H, Fernandez B and Christiansen O 1998 The benzene–argon complex: a ground and excited state *ab initio* study *J. Chem. Phys.* **108** 2784–90
[26] Koch H, Fernandez B and Makarewicz J 1999 Ground state benzene–argon intermolecular potential energy surface *J. Chem. Phys.* **111** 198–204
[27] Klopper W, Lüthi H P, Brupbacher Th and Bauder A 1994 *Ab initio* computations close to the one-particle basis set limit on the weakly bound van der Waals complexes benzene–neon and benzene–argon *J. Chem. Phys.* **101** 9747–54
[28] Lee S, Chung J S, Felker P M, Lopez Cacheiro J, Fernandez B, Petersen T B and Koch H 2003 Computational and experimental investigation of intermolecular states and forces in benzene–helium van der Waals complex *J. Chem. Phys.* **119** 12956–64
[29] Pirani F, Bartolomei M, Aquilanti V, Scotoni M, Vescovi M, Ascenzi D, Bassi D and Cappelletti D 2003 Collisional orientation of the benzene molecular plane in supersonic seeded expansions, probed by infrared polarized laser absorption spectroscopy and by molecular beam scattering *J. Chem. Phys.* **119** 265–76
[30] Pirani F, Porrini M, Cavalli S, Bartolomei M and Cappelletti D 2002 Potential energy surfaces for the benzene–rare gas systems *Chem. Phys. Lett.* **367** 405–13

[31] Pirani F, Albertí M, Castro A, Moix Teixidor M and Cappelletti D 2004 Atom-bond pairwise additive representation for intermolecular potential energy surfaces *Chem. Phys. Lett.* **394** 37–44
[32] Cappelletti D *et al* http://leo.tech.ing.unipg.it/PES/
[33] Johnson B R 1973 The multichannel log-derivative method for scattering calculations *J. Comput. Phys.* **13** 445–9
[34] López-Durán D, Bodo E and Gianturco F A 2008 Aspin: an all spin scattering code for atom–molecule rovibrationally inelastic cross sections *Comput. Phys. Commun.* **179** 821–38
[35] Hutson J M and Green S, MOLSCAT computer code, version 14 (1994), distributed by the Collaborative Computational Project No. 6 of the Engineering and Physical Science Research Council (UK)
[36] Bodo E and Gianturco F A 2003 Collisional cooling of polar diatomics in ^{3}He and ^{4}He buffer gas: a quantum calculation at ultralow energies *J. Phys. Chem.* A **107** 7328–36
[37] Bodo E and Gianturco F A 2006 Collisional quenching of molecular ro-vibrational energy by He buffer loading at ultra-low energies *Int. Rev. Phys. Chem.* **25** 313–51